

Supporting Information for

# Double Layer Composite Electrode Strategy for Efficient Perovskite Solar Cells with Excellent Reverse-Bias Stability

Chaofan Jiang<sup>1</sup>, Junjie Zhou<sup>1</sup>, Hang Li<sup>1</sup>, Liguo Tan<sup>1</sup>, Minghao Li<sup>1</sup>, Wolfgang Tress<sup>2</sup>, Liming Ding<sup>3</sup>, Michael Grätzel<sup>4</sup>, Chenyi Yi<sup>1,\*</sup>

<sup>1</sup>State Key Laboratory of Power System, Department of Electrical Engineering, Tsinghua University, Beijing, 100084, P. R. China

<sup>2</sup>Institute of Computational Physics (ICP) ZHAW School of Engineering Wildbachstr. 21, Winterthur 8400, Switzerland

<sup>3</sup>Center for Excellence in Nanoscience (CAS), Key Laboratory of Nanosystem and Hierarchical Fabrication (CAS), National Center for Nanoscience and Technology, Beijing, 100190, P. R. China

<sup>4</sup>Laboratory of Photonics and Interfaces, Department of Chemistry and Chemical Engineering, Swiss Federal Institute of Technology Lausanne, Lausanne CH-1015, Switzerland

\*Corresponding author. Email: [yicy@mail.tsinghua.edu.cn](mailto:yicy@mail.tsinghua.edu.cn) (Chenyi Yi)

## S1 Device Fabrication

The cleaned ITO glass substrates were treated with the UV-ozone before spin-coating SnO<sub>2</sub> solution (4000 rpm for 30 s). Afterwards, the substrates were annealed at 150 °C for 30 min in ambient air. Another UV-ozone was done before depositing perovskite films. The perovskite films were fabricated by typical two-step method according to our former report [S1]. We adopted the typical solution two-step method. The PbI<sub>2</sub> solution (1.5 M) was dissolved in mixed solvent (DMF/DMSO=9/1) and spun onto the SnO<sub>2</sub> films at 1500 rpm for 30 s and annealed at 70 °C for 1 min. Then the FAI/MAI/MACl (90mg/ 6.39mg/ 9mg) were dissolved in 1ml IPA and spun onto the PbI<sub>2</sub> films at 2000 rpm for 30 s. The perovskite thin films were annealed at 150 °C for 15 min in ambient air (30~40% RH). After cooling the perovskite films, devices were transferred into a N<sub>2</sub> glovebox. For perovskite surface treatment, PEAI solution in IPA was spin-coated onto the perovskite films at 4000 rpm for 20 s. Subsequently, a thin layer of hole transporting film was deposited by spin coating spiro-OMeTAD solution composed of 80 mg spiro-OMeTAD, 30 μL t-BP and 18 μL LiTFSI solution. Then, 10 nm MoO<sub>x</sub> was thermally evaporated as the buffer layer. For the composite electrode, indium tin oxide (ITO) was deposited onto MoO<sub>x</sub> by magnetron radio frequency (RF) sputtering with a cylindrical ITO target (10% SnO<sub>2</sub> and 90% In<sub>2</sub>O<sub>3</sub>) in Ar. We used a 4 inches target, 9 cm sample-to-target distance. The sputtering power was 100 W and the sputtering pressure was 1.5×10<sup>-3</sup> mbar. Finally, 100 nm of low-cost metal (Cu/Al/Ni) was thermally evaporated onto TCO to form the composite electrode.

S2 Supplementary Figures and Tables

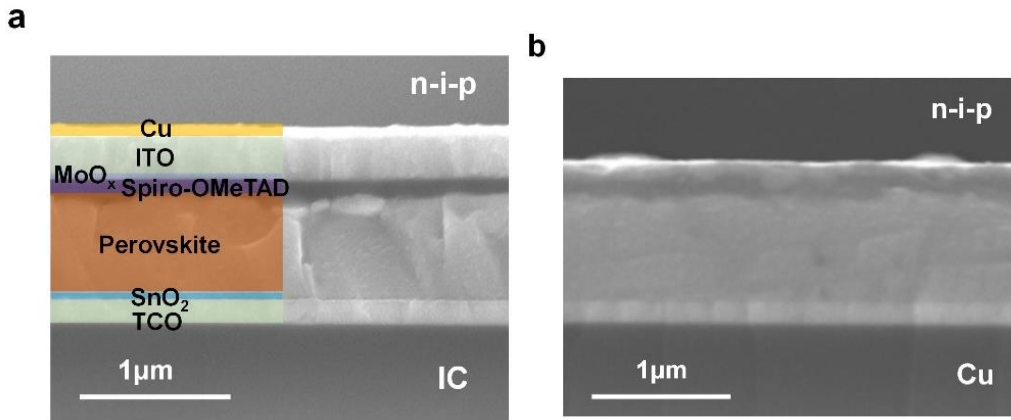


Fig. S1 (a) The cross-sectional SEM for IC-PSC. (b) The cross-sectional SEM for reference PSC

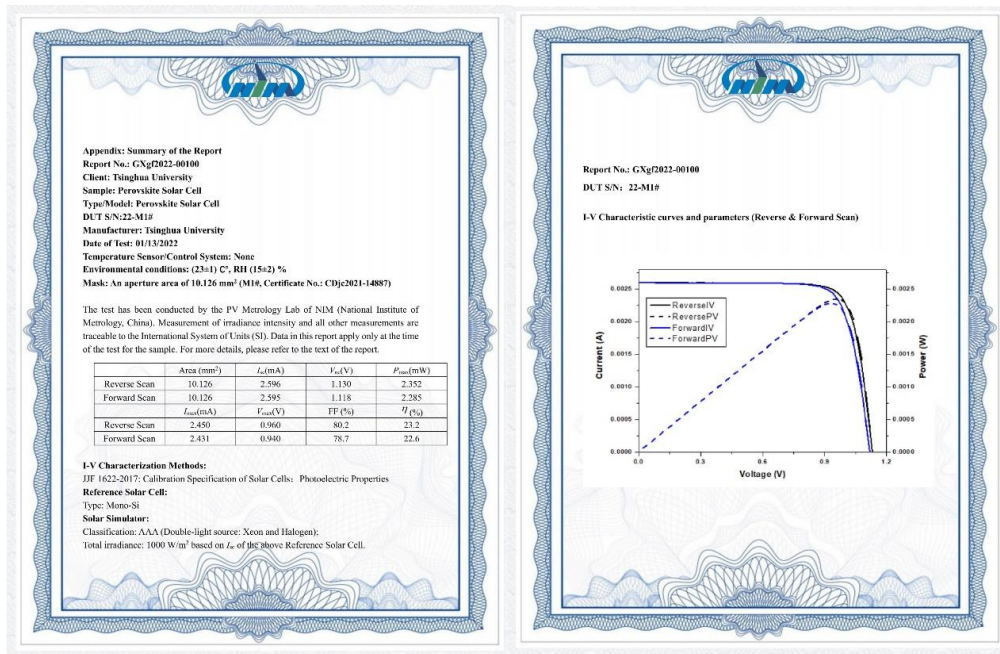
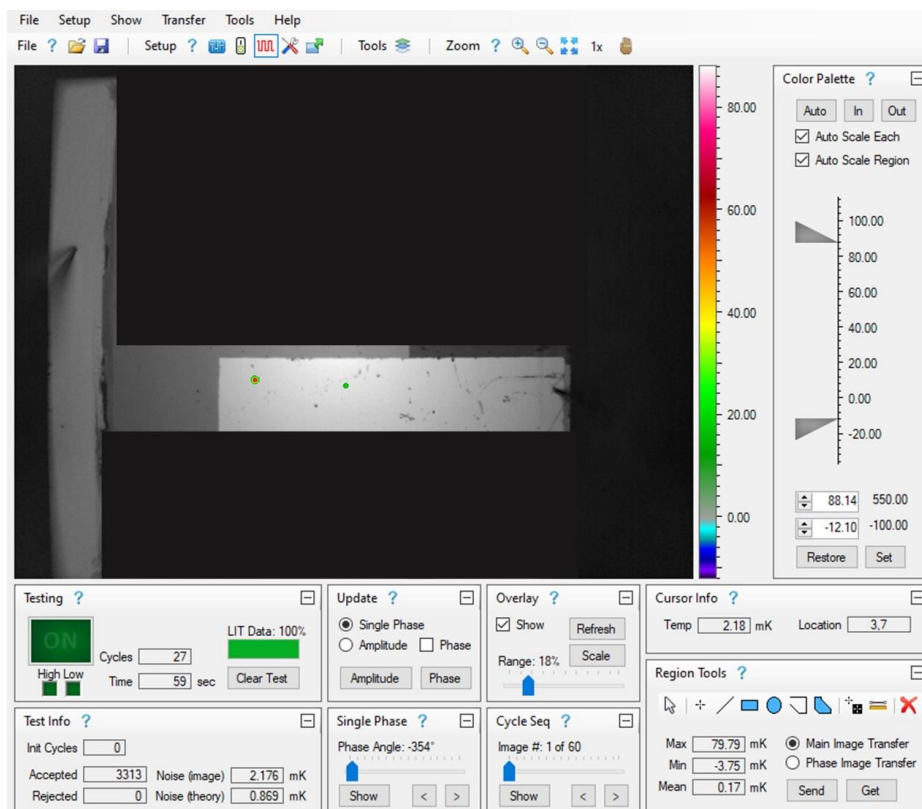
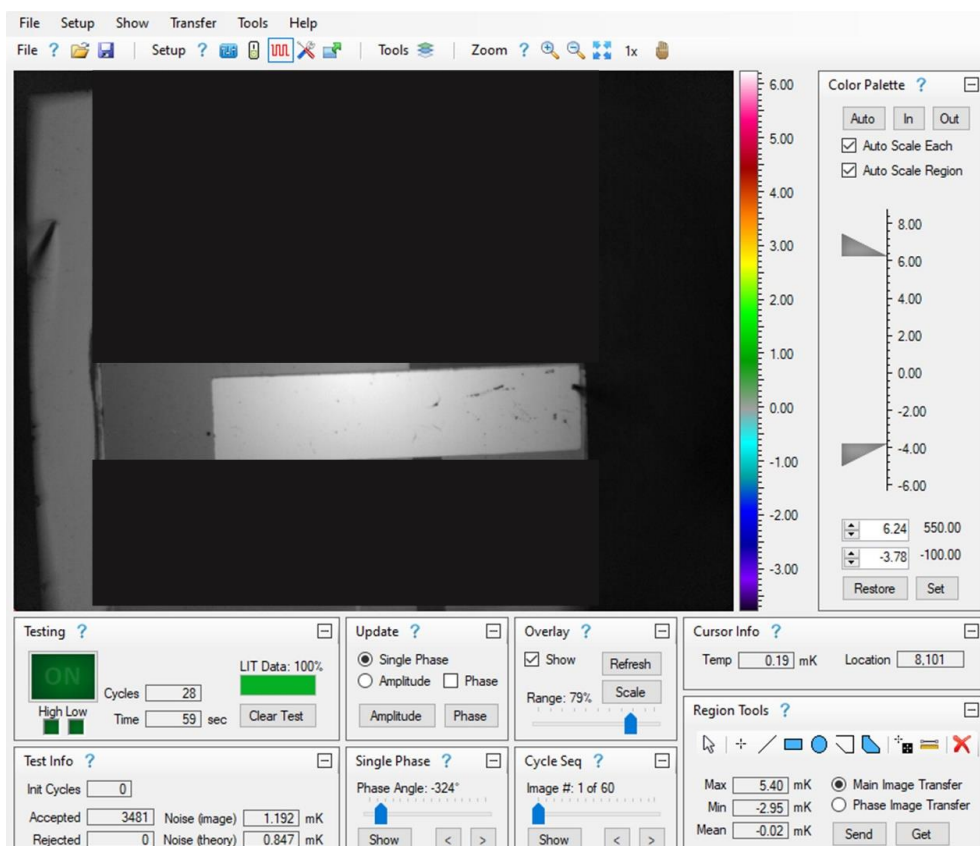


Fig. S2 Certification results of IC-PSCs by the National Institute of Metrology, China (NIM, China)



**Fig. S3** Thermal microscopy image for reference PSC. Test results (Pulse cycles: 27, Reverse bias voltage: 0.5 V, Leakage current: 1.2 mA, Maximum temperature increase: 79.79 mK)



**Fig. S4** Thermal microscopy image for IC-PSC. Test results (Pulse cycles: 28, Reverse bias voltage: 1 V, Leakage current: 28 nA, Maximum temperature increase: 5.40 mK)

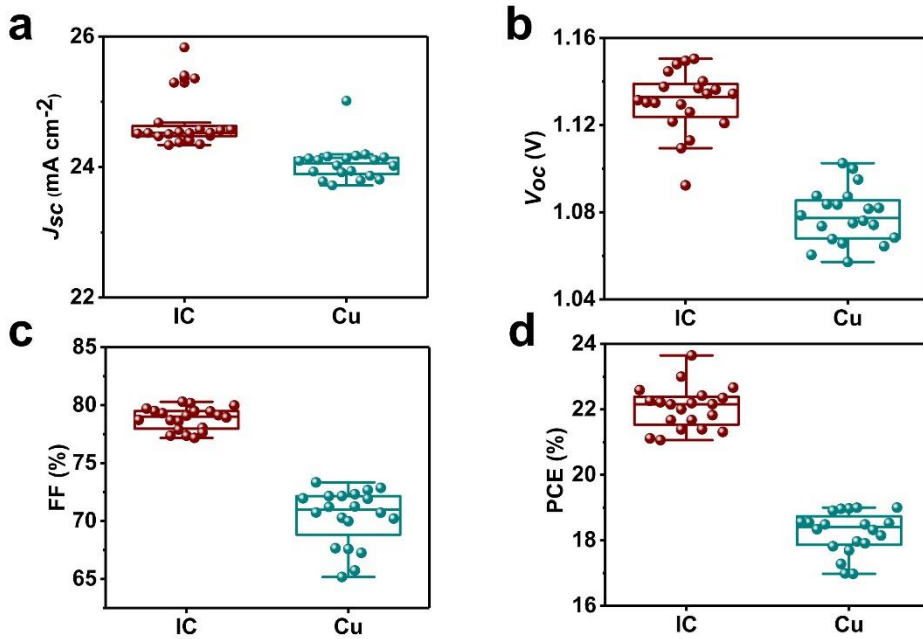


**Fig. S5** Device performance metrics statistics (a)  $J_{sc}$ , (b)  $V_{oc}$ , (c) FF, (d) PCE for IC-PSCs and reference PSCs

We fabricated three ITO films with different thicknesses, namely 100, 300 and 500 nm. As shown in Table. 1, the 100 nm ITO showed a relatively low mobility and high sheet resistance; and the 500 nm ITO showed a comparable resistance to 300 nm ITO. Compared with 300 nm ITO, the 500 nm ITO film exhibited a lower mobility and higher carrier concentration, contributing to a stronger absorption of light, which is unfavorable for the light management of PSCs. As a result, best PCE has been achieved with the PSCs based on 300 nm ITO and 100 nm copper as the composite electrode.

**Table S1** ITO thickness optimization results

ITO thickness (nm)	Sheet resistivity ( $\Omega/\square$ )	Mobility (cm <sup>2</sup> /V s)	Sheet carrier concentration (1/cm <sup>2</sup> )	Average PCE
100±10	2753	1.30	1.74E+14	20.83
300±10	93.63	14.71	4.53E+15	22.05
500±10	94.12	10.94	6.06E+15	21.43

We measured the transmittance (T%) for optimized ITO thin film. It is obvious that the film has 76.16% average transmittance from 300 to 900 nm and T% has covered the 80% and approached the 95% at the wavelength of 650 nm.

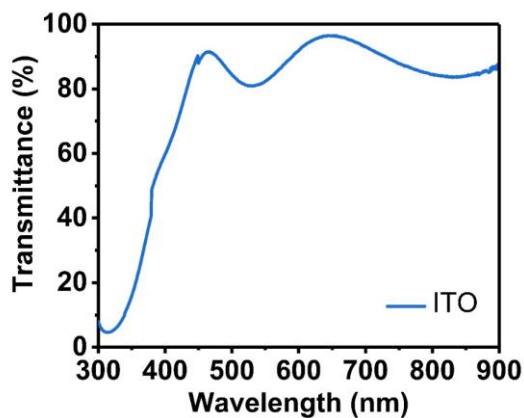


Fig. S6 Transmittance of optimized ITO film

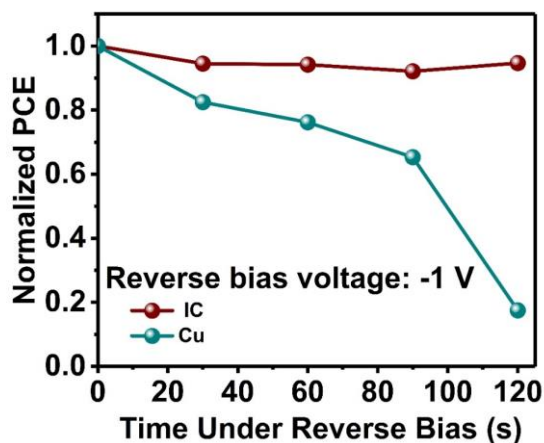


Fig. S7 Reverse-bias stability of the IC-PSC and reference PSC

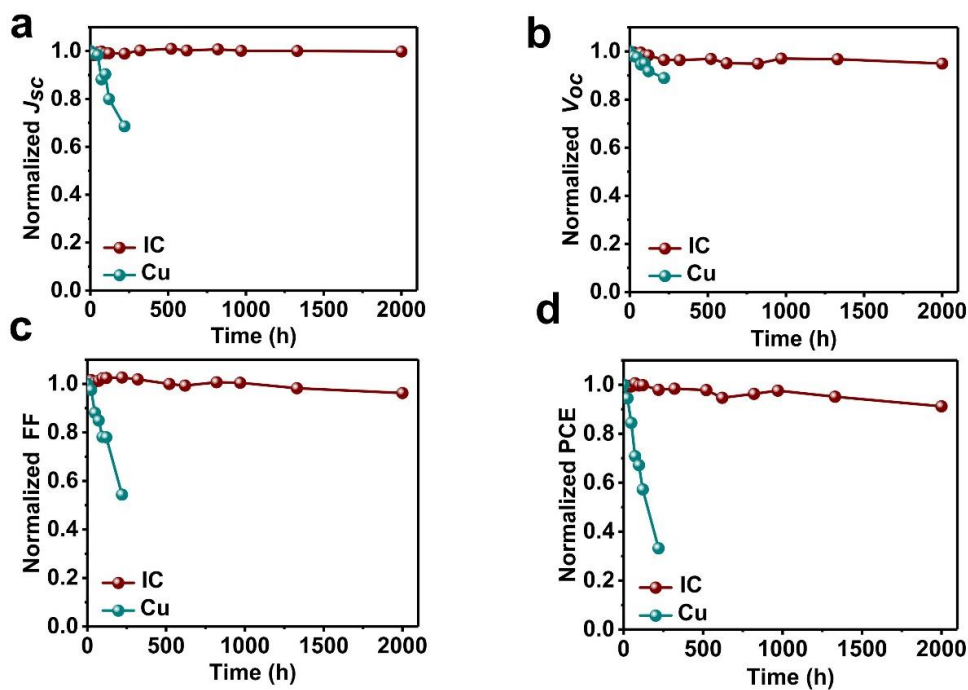
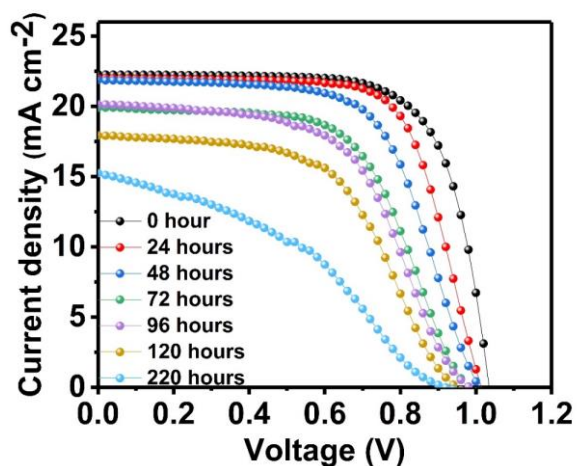
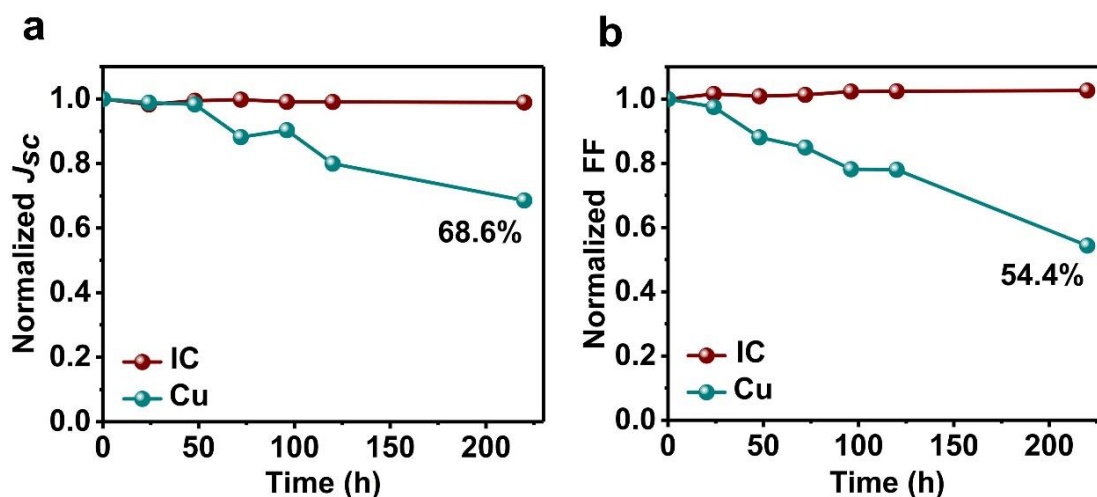


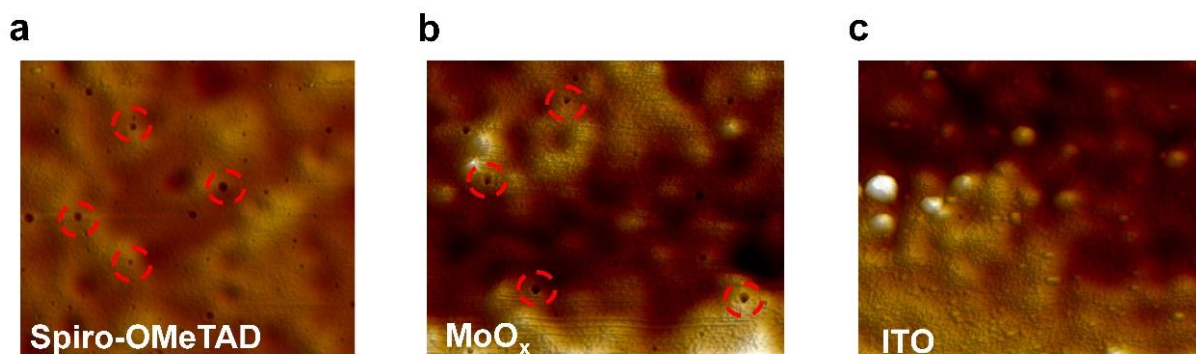
Fig. S8 Photovoltaic performance metrics for devices stored on the shelf. (a) normalized  $J_{sc}$ , (b) normalized  $V_{oc}$ , (c) normalized FF, (d) normalized PCE for IC-PSC and reference PSC



**Fig. S9** The  $J$ - $V$  curves for the reference device stored on the shelf (from 0 to 220 hours)



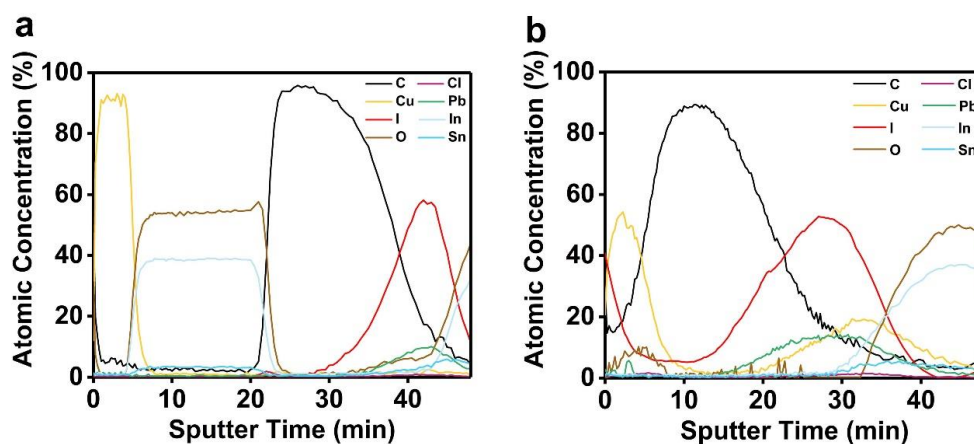
**Fig. S10** The key metrics performance changes (a) short-circuit current density and (b) fill factor of the PSCs in the first 220 h



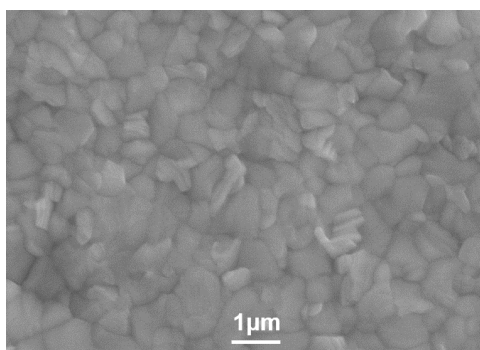
**Fig. S11** The 3D visual AFM for the (a) Spiro-OMeTAD, (b)  $\text{MoO}_x$  and (c) ITO surface morphology

**Table S2** The formation enthalpy ( $\Delta_f H$ ) and the free energy  $\Delta E (E_{M-M} - E_{M-I})$  of AuI; AgI and CuI [S2]

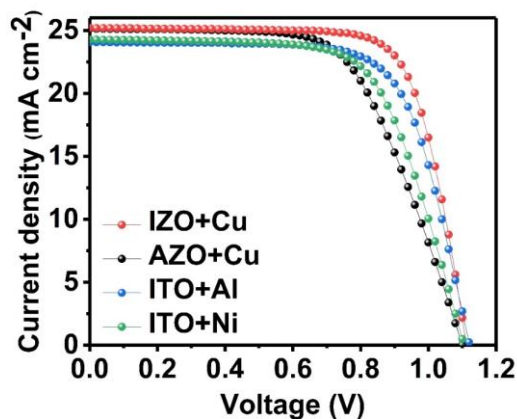
	$\Delta_f H$	$\Delta E$
AuI	0 kJ mol <sup>-1</sup>	-49.8 kJ mol <sup>-1</sup>
AgI	-61.8 kJ mol <sup>-1</sup>	-71.1 kJ mol <sup>-1</sup>
CuI	-68.7 kJ mol <sup>-1</sup>	-88 kJ mol <sup>-1</sup>



**Fig. S12** AES depth element profiling for aged (a) IC-PSC and (b) reference PSC after 1000 hours MPPT



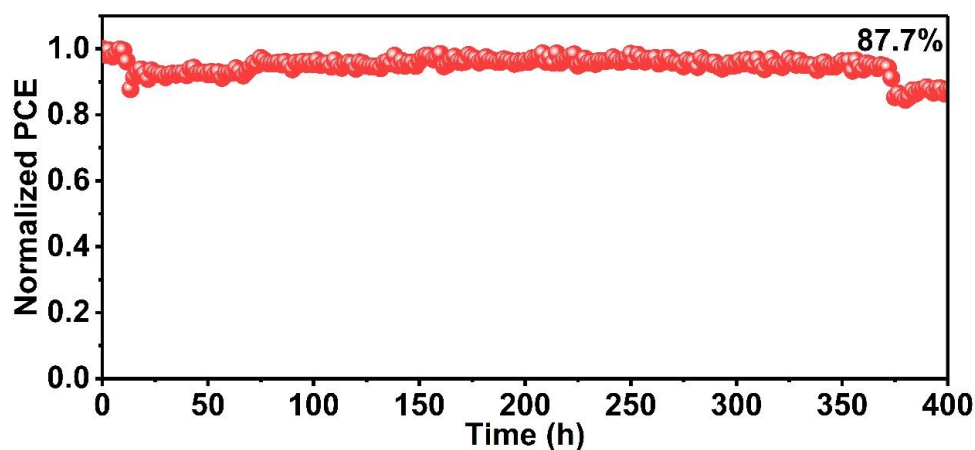
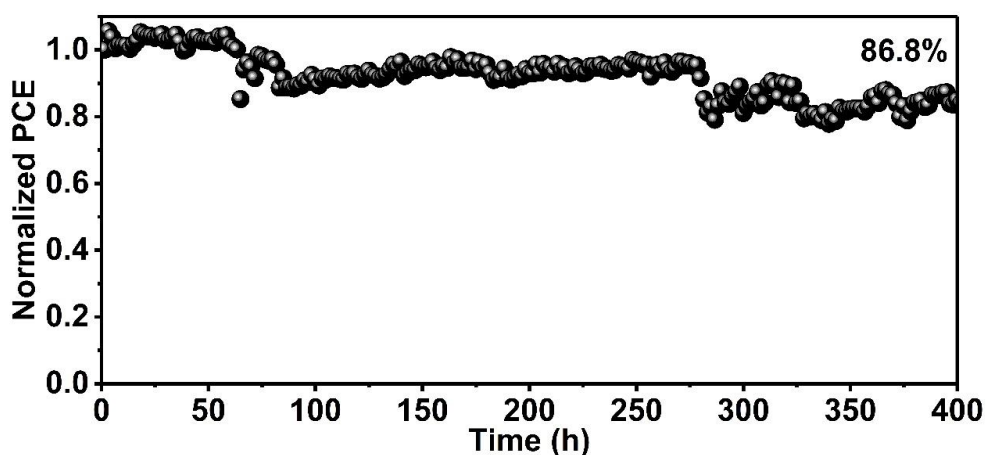
**Fig. S13** SEM images of the fresh perovskite film



**Fig. S14** The PSCs J-V curves based on different composite electrodes

**Table S3** Photovoltaic performance of the PSCs based on different composite electrodes

Device	$J_{sc}$ ( $\text{mA cm}^{-2}$ )	$V_{oc}$ (V)	FF (%)	PCE (%)
TCO/SnO <sub>2</sub> /Perovskite/SpiroOMeTAD/MoO <sub>x</sub> /IZO+Cu	25.19	1.11	73.97	20.7
TCO/SnO <sub>2</sub> /Perovskite/SpiroOMeTAD/MoO <sub>x</sub> /AZO+Cu	25.19	1.10	61.85	17.1
TCO/SnO <sub>2</sub> /Perovskite/SpiroOMeTAD/MoO <sub>x</sub> /ITO+Al	24.06	1.12	69.99	18.9
TCO/SnO <sub>2</sub> /Perovskite/SpiroOMeTAD/MoO <sub>x</sub> /ITO+Ni	24.25	1.10	66.20	17.7

**Fig. S15** The MPP tracking performance of the unencapsulated PSCs with IZO+Cu composite electrode under continuous illumination (white LED lamp). The initial PCE was 20.2%**Fig. S16** MPP tracking performance of the unencapsulated PSCs with AZO+Cu composite electrode under continuous illumination (white LED lamp)



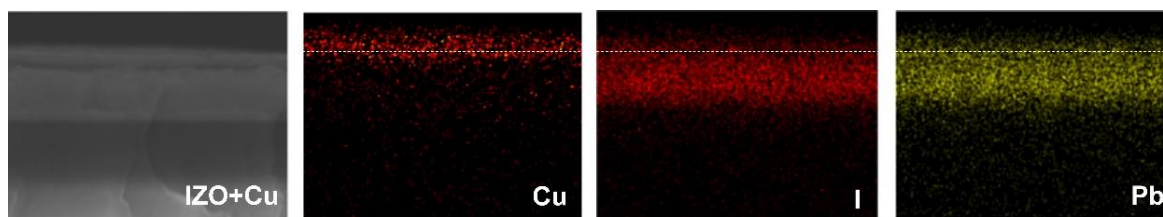


**Fig. S17** Cross-section EDX mapping of Cu, I, and Pb elements for PSCs with IZO+Cu composite electrode

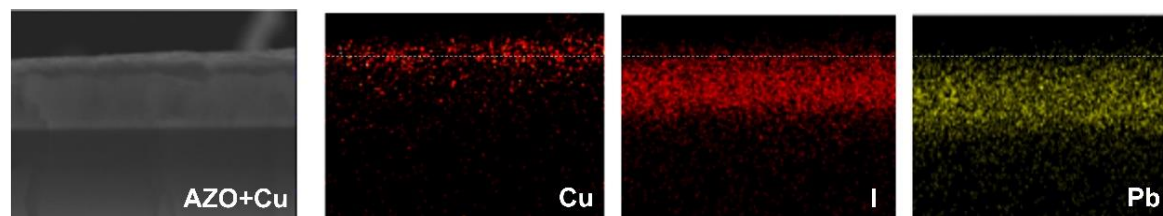


**Fig. S18** Cross-section EDX mapping of Cu, I, and Pb elements for PSCs with AZO+Cu composite electrode

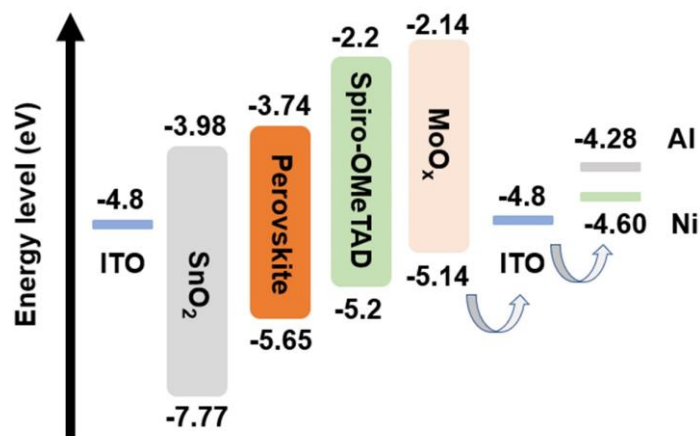


**Fig. S19** Energy level matching diagram for PSCs with different metal electrode layer aluminum (Al) and nickel (Ni)

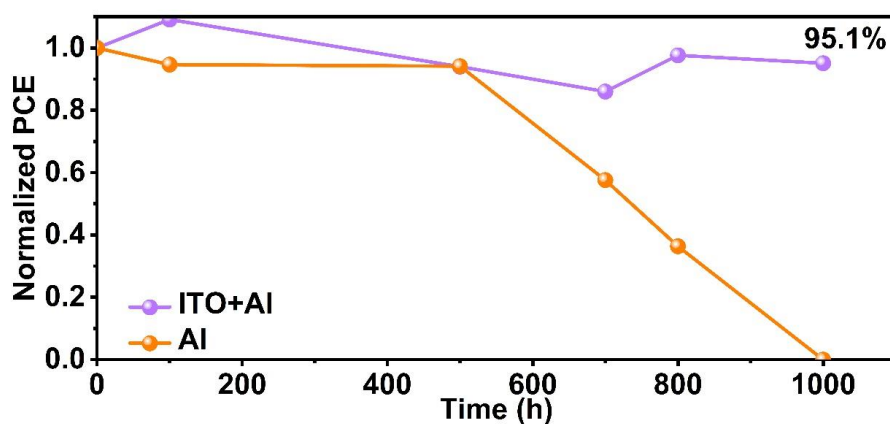


**Fig. S20** Device shelf life stability performance for PSCs with ITO+Al composite electrode and reference PSCs

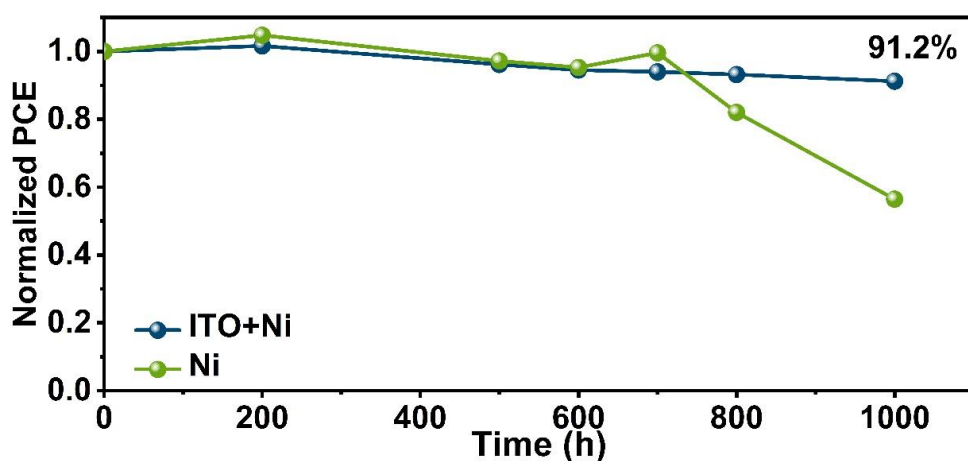


**Fig. S21** Device shelf life stability performance for PSCs with ITO+Ni composite electrode and reference PSCs

### Supplementary References

- [S1] M. Li, J. Zhou, L. Tan, Y. Liu, S. Wang et al. Brominated PEAI as multi-functional passivator for high-efficiency perovskite solar cell. *Energy Environ. Mater.* (2022). <https://doi.org/10.1002/eem2.12360>
- [S2] S. Wu, R. Chen, S. Zhang, B.H. Babu, Y. Yue et al. A chemically inert bismuth interlayer enhances long-term stability of inverted perovskite solar cells. *Nat. Commun.* **10**, 1161 (2019). <https://doi.org/10.1038/s41467-019-09167-0>